Fermi-surface studies in the two-dimensional organic conductors $(BEDT\text{-}TTF)_2MHg(SCN)_4$ (M=Tl,K,Rb,NH_4)

S. Uji, T. Terashima, and H. Aoki
Tsukuba Magnet Laboratories, National Research Institute for Metals, Tsukuba, Ibaraki 305, Japan

J. S. Brooks
Department of Physics, Florida State University, Tallahassee, Florida 32306-4005

M. Tokumoto, N. Kinoshita, T. Kinoshita, and Y. Tanaka
Electrotechnical Laboratory, Tsukuba, Ibaraki 305, Japan

H. Anzai
Himeji Institute of Technology, Akahogun, Hyogo 678-12, Japan
(Received 15 January 1996; revised manuscript received 11 June 1996)

The Shubnikov–de Haas (SdH) measurements of the two-dimensional organic conductors $(BEDT\text{–}TTF)_2MHg(SCN)_4$ for M=Tl, K, Rb, and NH_4 have been performed in order to investigate the structure of the Fermi surface. In addition to the closed orbit and the magnetic breakdown orbit in the original Fermi surface, many different SdH oscillations are found for the salts (M=Tl, K, and Rb) which have the spin-density-wave (SDW) ground state whereas only one frequency is observed for the NH_4 salt. All the frequencies follow the same angular dependence. On the basis of the relation between the SdH frequencies, the Fermi surface in the SDW phase, which has no open sheets, is reconstructed. The origin of the magnetic breakdown orbit and the large hysteresis in the resistance observed below the transition field for M=Tl, K, and Rb is explained in terms of the coexistence of the SDW phase and the normal metallic phase. [S0163-1829(96)01637-2]

I. INTRODUCTION

Charge-transfer salts of the form $(BEDT\text{-}TTF)_2X$, where BEDT-TTF is bis(ethylenedithio)tetrathiafulvalene, have been extensively studied in order to understand the ground states in low-dimensional systems. Among the various salts of the (BEDT-TTF) family, $(BEDT\text{-}TTF)_2MHg(SCN)_4$ (M=K,Tl,Rb,NH_4) salts have been of particular interest due to the low-temperature properties.

The NH_4 salt in the $(BEDT\text{-}TTF)_2MHg(SCN)_4$ family shows the superconductivity at about 1 K.[1] However, the other salts (M=K,Tl,Rb) are metallic down to 50 mK, and show a magnetic phase transition at low temperatures (T_N=8–12 K).[2–6] The ground states of the salts (M=K,Tl, Rb) have been suggested to be spin-density-wave (SDW) states[7] from the magnetic-susceptibility[8,9] and the electron-spin-resonance measurements.[10] A BCS-like jump in the heat capacity is also observed at T_N for the K and Rb salts.[11] The phase diagram for the K, Tl, and Rb salts is shown in Fig. 1.[3] For the K salt, the SDW phase is removed by a high field of about 23 T (H_K), where the kink behavior in the magnetoresistance is seen.[2–4,12–15] A large hysteresis in the magnetization and the magnetoresistance has been observed in the SDW phase, and the presence of the additional phase line (H_A) in the SDW phase is proposed.[3] The possibility of the filamentary superconductivity in the SDW phase,[16] and the superconductivity induced by the uniaxial stress have been reported at low fields for the K or Rb salts.[17]

According to the band-structure calculation, the $(BEDT\text{-}TTF)_2MHg(SCN)_4$ in the normal metallic (M) phase has one-dimensional (1D) and 2D Fermi surfaces (FS's).[18] The schematic picture of the FS's in the most conducting plane (ac plane) is shown in Fig. 1. For the K, Tl, and Rb salts, the SDW transition is considered to be caused by the nesting of the two sheets of the 1D FS. The nesting causes the reconstruction of the FS and the models of the reconstructed FS have been proposed by several groups.[19–22]

Kartsovnik, Kovalev, and Kushch[19] constructed the FS in

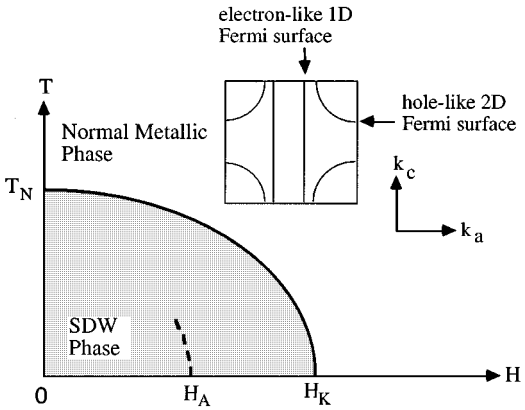

FIG. 1. Phase T-H diagram of $(BEDT\text{-}TTF)_2MHg(SCN)_4$ for M=Tl, K, and Rb. The schematic Fermi surface in the normal metallic phase is also shown. The SDW phase is removed by the magnetic field H_K. An additional phase line H_A in the SDW phase is shown by a broken line (Ref. 3). Hysteretic behavior in the magnetoresistance and the magnetization is observed in the field range between H_A and H_K.

the SDW phase on the basis of the angular-dependent magnetoresistance oscillation (ADMRO) and the Shubnikov–de Haas (SdH) oscillations. In their model, there exist 2D and 1D FS's, which have a lens orbit and an open orbit along the nesting vector, respectively. In this case, the observed two SdH oscillations are assigned to the lens orbit and the magnetic breakdown (MB) orbit. The MB orbit is exactly the same as the closed orbit on the original 2D FS in the M phase. The anomalous ADMRO results observed in the SDW phase are explained in terms of the drift motion of the conduction electrons on the reconstructed 1D FS. Similar models of the reconstructed FS have been proposed by other groups.[20–22] These models are apparently based on the fact that two fundamental SdH oscillations are observed in the SDW phase. Such a reconstructed FS is obtained when the cross section of the original 2D FS is assumed to have a circular shape in the ac plane. However, the cross section of the original 2D FS is determined to be an elongated ellipse rather than a circle from the observation of the standard ADMRO in the M phase.[19,20,22] When the 2D FS has an elliptical cross section, the reconstructed FS has a more complicated topology than the simple models. We have observed many SdH oscillations for the Tl salt,[23] some of which have not been reported by the other groups. The observation of these oscillations clearly suggests that the reconstructed FS is more complicated than their models.

To investigate the complete structure of the FS, we have made extensive magnetoresistance and SdH measurements on the (BEDT-TTF)$_2M$Hg(SCN)$_4$ salts (M=K, Tl, Rb, and NH$_4$) over broad ranges of magnetic field and temperature. The various SdH oscillations for M=K, Tl and Rb have been detected down to 0.2 T by means of a field modulation technique. The SdH data shows that the K, Tl, and Rb salts have complicated FS's in the SDW phase. For the NH$_4$ salt, only one SdH oscillation is found, which shows that the FS has a simple structure as predicted by the band calculation.

II. EXPERIMENT

(BEDT-TTF)$_2M$Hg(SCN)$_4$ single crystals were grown electrochemically. The single crystals are platelet and the ac plane is the most conducting plane. Using gold paint, gold wires (ϕ10 μm) were attached on a face (ac plane) of the platelets for the in-plane resistance measurements, and on both the faces for the measurements along the b^* axis. To avoid sample heating, the dc currents were selected to be in the range between 1 and 100 μA. The samples were directly mounted in the ^{3}He-^{4}He mixture of the dilution refrigerator. The temperature of the sample was controlled by using a carbon resistor and a resistance heater in the mixing chamber. The SdH signals were measured by a standard low-frequency field modulation technique in the frequency range from 17 to 37 Hz. All the SdH signals were detected at the second harmonic of the modulation frequency for the current perpendicular to the conduction plane.

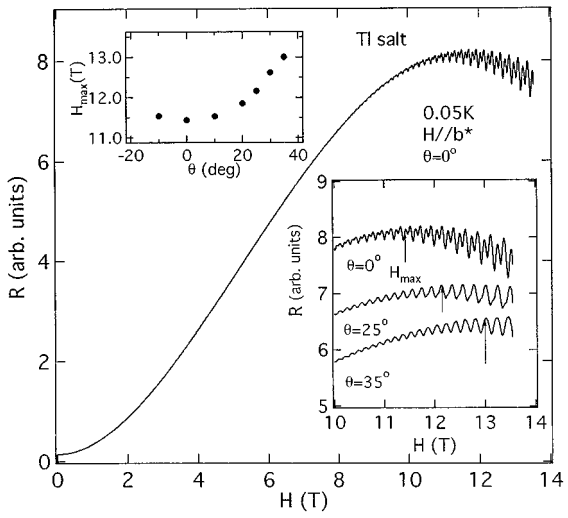

FIG. 2. Resistance at 0.05 K for the Tl salt. The angular dependence of H_{max} and the resistance in a high-field region are shown in the insets. θ is the angle between the b^* axis and the magnetic field.

III. EXPERIMENTAL RESULTS

A. Magnetoresistance

The in-plane resistance at 0.05 K for the Tl salt is presented in Fig. 2. θ is the angle between the magnetic field and the b^* axis. The SdH oscillations are evident above 10 T. In this data, only one SdH oscillation (denoted by α_1 later) and its second harmonic are evident. The nonoscillatory background of the resistance increases with field and shows a maximum around 11 T. The field where the resistance has the maximum H_{max} is denoted by the arrows in the inset. H_{max} increases as the field is tilted from the b^* axis to the ac plane. Similar resistance maxima have been observed for the K and Rb salts.

Figure 3 shows the in-plane resistance for the NH$_4$ salt. The zero resistance due to the superconductivity is seen in a low-field region. A SdH oscillation is seen above 8 T. In contrast to the results for the Tl salt, we cannot observe a resistance maximum for the NH$_4$ salt. Osada *et al.* report that the magnetoresistance monotonically increases with field up to 30 T.[24] The resistance maximum is observed only for the salts which have the SDW ground state. The correlation between the resistance maximum and the SDW ground state will be discussed in Sec. IV.

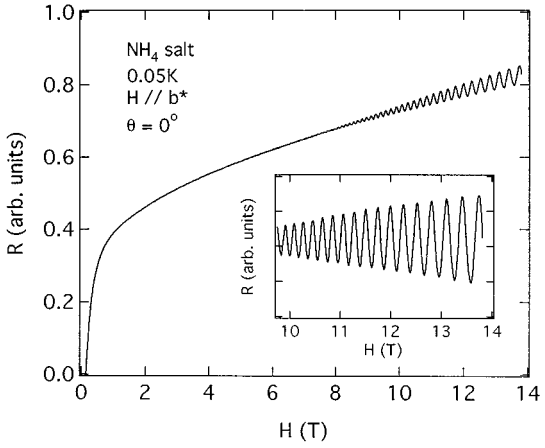

FIG. 3. Resistance at 0.05 K for the NH$_4$ salt. The superconducting transition is seen at low fields below 0.2 T. The oscillatory part of the resistance in a high-field region is shown in the inset.

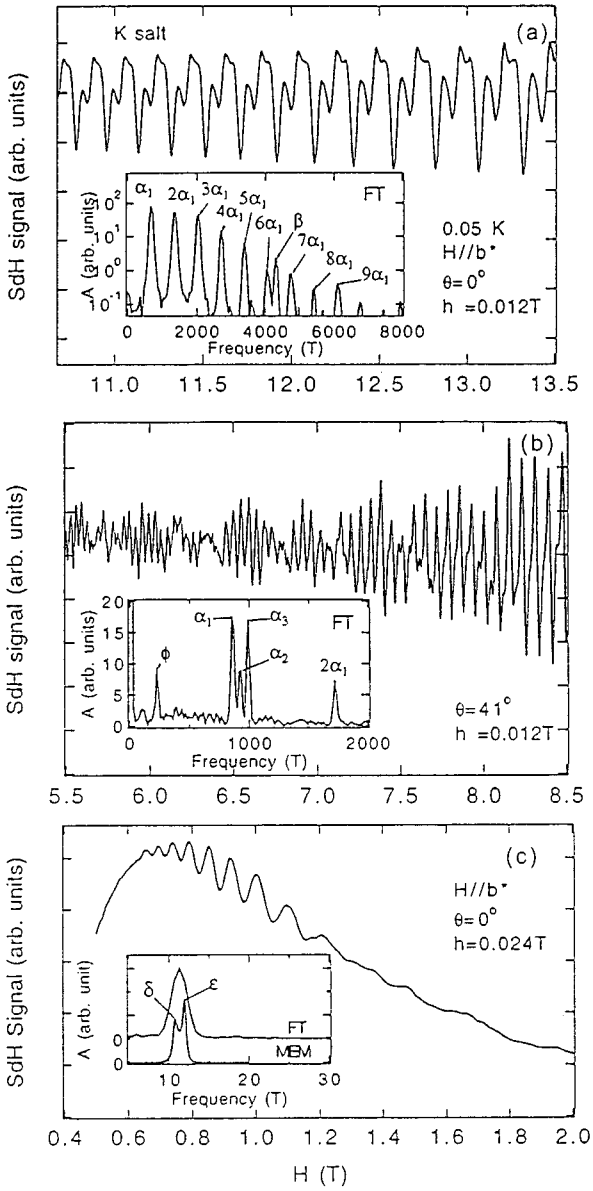

FIG. 4. SdH signals at 0.05 K in various magnetic field ranges for the K salt. The modulation field h is 0.012 or 0.024 T. The FT and/or MEM spectra of the signals are shown in the insets.

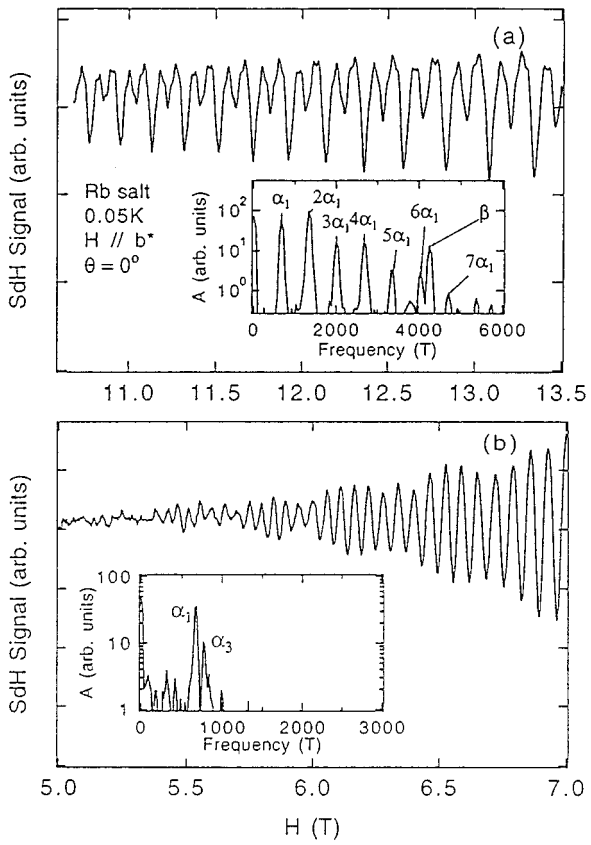

FIG. 5. SdH signals at 0.05 K in two different magnetic-field ranges ($H//b^*$) for the Rb salt. The modulation field is 0.018 T. The FT spectra of the signals are shown in the insets.

B. SdH oscillations

Figures 4(a)–4(c) show the SdH oscillations measured at 0.05 K for the K salt. In the highest magnetic field region [Fig. 4(a)], two fundamental oscillations α_1 and β are evident in the Fourier transform (FT) spectrum [inset of Fig. 4(a)]. The α_1 oscillation [F (α_1)=673 T], which is in good agreement with the reported value, is assigned to the closed orbit on the 2D FS predicted by the band calculation [Fig. 1(a)]. The β oscillation is assigned to the MB orbit,[35] whose cross-sectional area corresponds to ~100% of the Brillouin zone in the ac plane. The two oscillations α_1 and β are also observed at high fields for the Tl salt[23] and Rb salt [Fig. 5(a)].

Generally, the signal-to-noise ratio is greatly improved by the field modulation technique. For the second-harmonic detection of the modulation frequency, the observed oscillation amplitude is multiplied by a factor $J_2(2\pi fh/H^2)$, where J_2 is the second-order Bessel function. The variables, f, h, and H are the SdH frequency, the modulation amplitude, and the external magnetic field, respectively. The data in Fig. 4(a) is taken so that the high-frequency oscillations for $F \approx 4000$ T are detected predominantly than the other oscillations by selecting the suitable modulation amplitude. This is probably the main reason why β is easily seen by the field modulation technique. Recently, Brooks *et al.* observed β by the conventional magnetoresistance measurements and found that the relative amplitude is enhanced by the pressure.[25]

The observation of α_1 and β is consistent with the calculated band structure shown in Fig. 1. Therefore, the results seem to suggest that the FS is not (at least partially) reconstructed in this field region, which will be discussed in Sec. IV.

Below 10 T [Fig. 4(b)], we find other oscillations α_2, α_3, and ϕ for the K salt. The amplitudes of these oscillations are much smaller than those of α_1 and β at higher fields. The similar oscillations are observable for the Rb salt [Fig. 5(b)]. For the Tl salt, the η and κ oscillations are observed in addition to α_2, α_3, and ϕ in this field region.[23]

In Fig. 4(c), the low-frequency oscillations δ and ϵ are presented for the K salt. The power spectrum is calculated by the maximum entropy method[26] (MEM) to improve the resolution [inset of Fig. 4(c)]. The lowest frequency oscillation γ (Ref. 27) is not evident for the K salt, but the Tl salt clearly shows the γ oscillation.[23]

For the Rb salt, α_3, η, κ, and ϕ are not evident. The frequencies of all the observed oscillations for $H//b^*$ are listed in Table I. The relative amplitudes of all the oscilla-

TABLE I. Frequencies and cyclotron masses of the SdH oscillations for $H//b^*$ axis in (BEDT-TTF)$_2$MHg(SCN)$_4$ (M=K,Tl,Rb,NH$_4$).

	Tl		K		Rb		NH_4	
Label	$F(T)$	m_c/m_0	$F(T)$	m_c/m_0	$F(T)$	m_c/m_0	$F(T)$	m_c/m_0
γ	1.2	0.23	b	b	b	b	b	b
δ	11.2	a	10.8	a	b	b	b	b
ε	12.6	a	11.6	a	b	b	b	b
η	38	a	b	b	b	b	b	b
κ	69	a	b	b	b	b	b	b
ϕ	183	2.0	180	1.4	b	b	b	b
α_1	664	1.4	673	1.5	672	1.5	565	2.5
α_2	720	1.6	720	a	b	b	b	b
α_3	768	2.0	777	1.9	773	1.9	b	b
β	4261	3.8	4260	3.7	4265	4.0	b	b

[a]Not measured.
[b]Not found.

tions (α_1,α_2,α_3,β,...) are sample dependent, but the frequencies are sample independent. The sample dependences of the amplitudes may be due to the sample quality and/or the local stress due to the sample cooling process.

These many oscillations are observable only for the salts which have the SDW ground states (M=K, Tl, and Rb). This fact shows that the observed oscillations are closely related to the reconstruction of the FS due to the SDW formation.

A lot of the SdH studies have been done for these salts by many groups. They have carried out the experiments at relatively high fields ($H>10$ T), where the oscillations (α_2, α_3, γ, δ, and ε) have small amplitudes. Low-field measurements by the field modulation technique are necessary for the observation of these oscillations.

In Fig. 6, the SdH oscillation is presented at 0.05 K for the NH_4 salt. Although we carefully measured the oscillations, we could not detect any other oscillations except α_1 and its harmonics. The frequency of α_1 (F=565 T) for the NH_4 salt is smaller than those for the other salts ($F\approx$670 T). The oscillation amplitude of α_1 decreases with increasing field in Fig. 6. This is caused by the field dependence of the Bessel function factor J_2 due to the second-harmonic detection.[28]

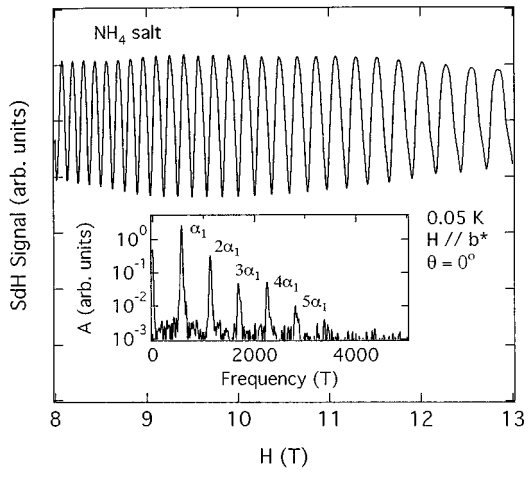

FIG. 6. SdH signal at 0.05 K at high fields ($H//b^*$) for the NH_4 salt. The modulation field is 0.018 T. The FT spectrum of the signal is shown in the inset.

The absence of the β oscillation is closely related to the MB probability. The MB probability p at the Brillouin-zone boundary in the M phase[28] is

$$p=\exp(-H_0/H), \qquad H_0\cong\frac{m_c c}{\hbar e}\frac{E_g^2}{E_F}, \tag{1}$$

where E_g and E_F are the energy gap between the two energy bands and the Fermi energy, respectively. m_c is the effective mass. The cross-sectional area of the 2D FS corresponding to α_1 for the NH_4 salt is smaller than those for the other salts. This fact means that the energy gap E_g between the closed and open orbits for the NH_4 salt is larger than that for the other salts. On the other hand, the effective mass m_c of α_1 for the NH_4 salt is about 1.6 times heavier than that of other salts as shown later. Both the facts suppress the MB, which explains the absence of β for the NH_4 salt.

C. Angular dependence of the frequencies

The angular dependences of the SdH frequencies for the K and NH_4 salts are presented in Fig. 7. We find that all of them follow the $1/\cos\theta$ dependence, where θ is the angle between the magnetic field and the b^* axis. The same angular dependence is also found for the Tl and Rb salts. The fairly good agreement with the $1/\cos\theta$ dependence shows that all the FS's corresponding to the oscillations have nearly cylindrical shapes.

D. Field dependence of the oscillation amplitude

To investigate the field dependence of each oscillation, we have performed the FT within 0.17 T^{-1} range of the inverse magnetic field. The FT spectra in various field regions for the Tl salt are presented in Fig. 8. H_{cf} means the center of the field range where the FT is performed. For H_{cf}=10.46 T, we can slightly see α_3, β, and ϕ in addition to α_1 and its harmonics. As the field decreases, α_3 and ϕ become evident. The α_2 oscillation cannot be well resolved from α_1 and α_3 because of the limited FT field range.

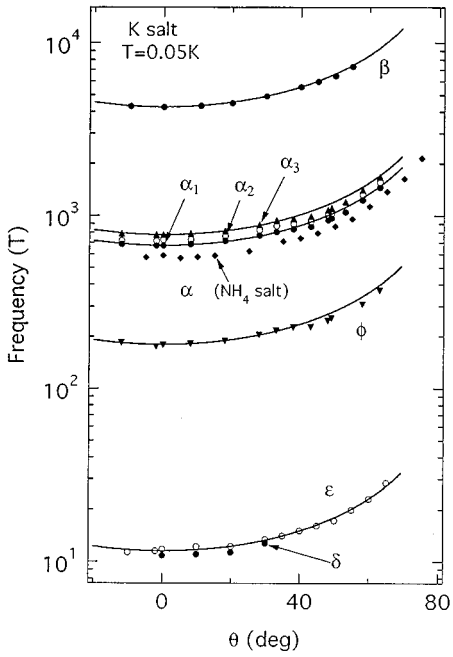

FIG. 7. Angular dependences of the SdH frequencies at 0.05 K for the K and NH_4 salts. The solid lines show the $1/\cos(\theta)$ dependences.

The field dependence of the amplitudes of α_1, $2\alpha_2$ (second harmonic of α_2), α_3, β, and ϕ above 4 T are presented in the inset of Fig. 8. Each FT amplitude is divided by the Bessel function factor J_2 (Ref. 28) to obtain the relative amplitude correctly. For γ, δ, and ε, the oscillation amplitudes

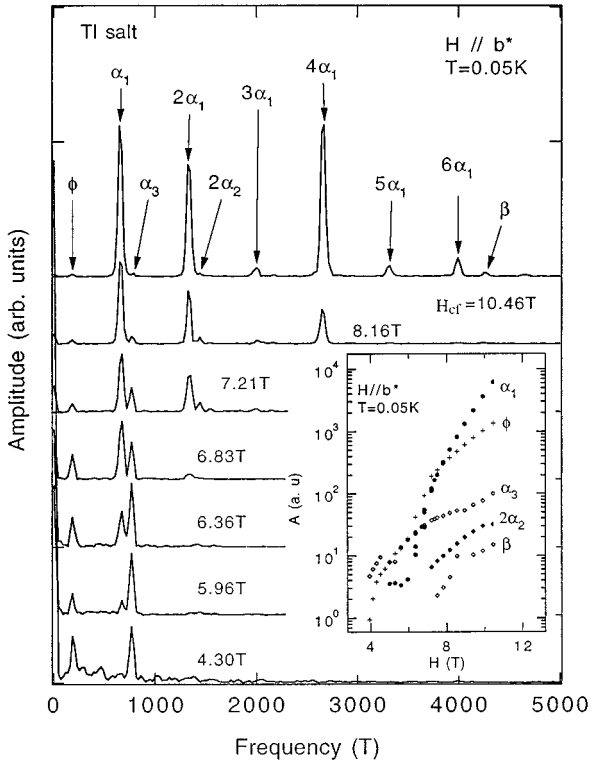

FIG. 8. FT spectra calculated within 0.17 T^{-1} range of the inverse magnetic field for the Tl salt. H_{cf} means the center of the FT field range.

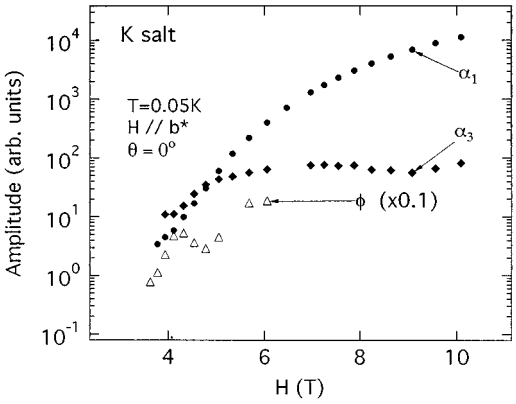

FIG. 9. Magnetic-field dependences of the oscillation amplitudes corrected by the Bessel function factor for the K salt.

show monotonic increase with increasing field.[23] The amplitude of α_1 shows anomalous behavior at ~6 T. The field dependences of the oscillation amplitudes for the K salt are shown in Fig. 9. Here, reliable data is not obtained for α_2, β, δ, and ε because of the small amplitudes. In contrast to the case for the Tl salt, an anomalous field dependence is seen at ~5 T for ϕ for the K salt. The anomalous behavior in the amplitude may be due to the field dependence of the nesting.[23]

E. Temperature dependence of δ and ε

Temperature dependence of the δ and ε oscillations for the K salt is shown in Fig. 10(a). The MEM spectra at various temperatures are presented in Fig. 10(b). For comparison, the results for the Tl salt at 0.1 K are shown by the dotted lines. We find that the frequencies of both the oscillations approach each other as temperature increases, and that they cannot be resolved above 0.13 K. The temperature dependences of the frequencies and the oscillation amplitudes are presented in Figs. 11(a) and 11(b). The amplitude is obtained from the FT spectra because the amplitude is not generally reliable for MEM. The amplitude in Fig. 11(b) roughly shows the sum of the amplitudes of δ and ε since they are not resolved in the FT spectra. Similar temperature dependences for δ and ε are reported for the Tl salt,[27] which are shown by the dotted lines.

F. Effective mass

The effective masses of the oscillations were determined by the temperature dependences of the amplitudes [Figs. 12(a) and 12(b)]. The solid lines show the fitted results by Lifshits-Kosevich (LK) formula.[28] The effective masses of the oscillations for $H//b^*$ are listed in Table I. The masses of δ and ε cannot be determined because the frequencies are temperature dependent. The amplitudes of η and κ are very small so that the reliable values of their masses have not been obtained.

Figure 13 shows the mass plot for the NH_4 salt. We note that the effective mass of α_1 for the NH_4 salt is significantly heavier than those of other salts. This mass is consistent with the reported results.[29] This heavy mass has been discussed in terms of the mass enhancement due to many-body effects.[29]

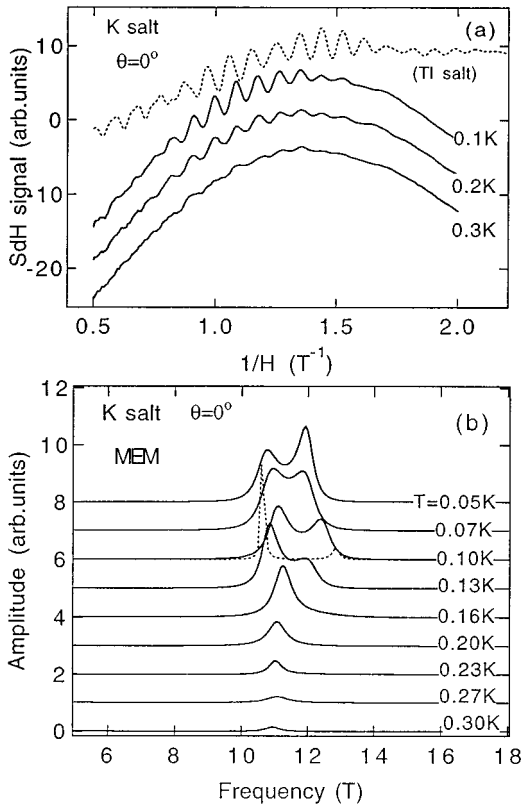

FIG. 10. (a) Low-field SdH signals at different temperatures for the K salt. (b) MEM spectra of the signals. The dotted lines are the results for the Tl salt at 0.1 K from Ref. 27.

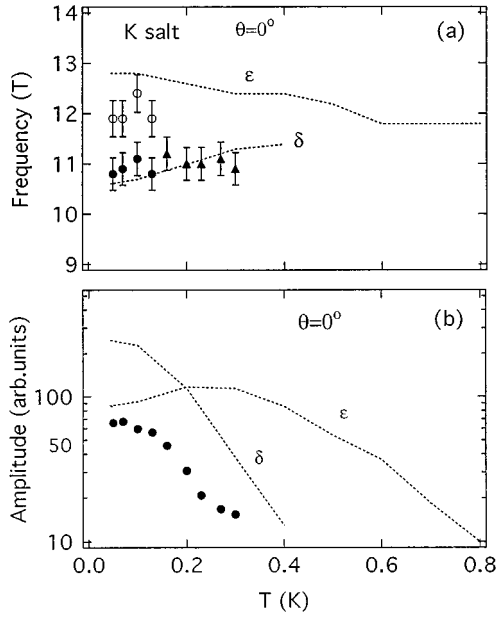

FIG. 11. (a) Temperature dependences of the low frequencies determined by the MEM for the K salt. (b) Sum of the oscillation amplitudes of δ and ε obtained from the FT spectra. The dotted lines are the results for the Tl salt from Ref. 27.

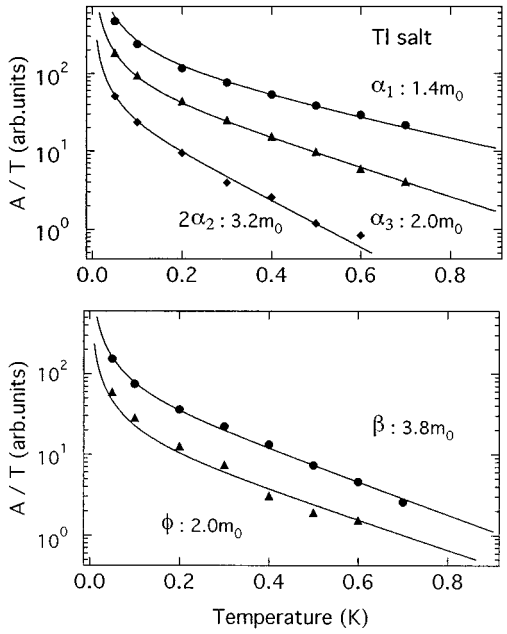

FIG. 12. Oscillation amplitude divided by temperature vs temperature for α_1, $2\alpha_2$, α_3, β, and ϕ for the Tl salt. The solid lines are the fitted results by the LK formula.

However, the reason why the many-body effects are strong only in the NH_4 salt is still an open question.

IV. DISCUSSION

We have found many oscillations in addition to α_1 and β in the SDW phase for the Tl, K, and Rb salts. These oscillations cannot be predicted from the band-structure calculation. The observation of many oscillations clearly demonstrates that the original FS is reconstructed in the SDW phase. On the other hand, the observation of α_1 and β at high fields suggest that the FS is consistent with the calculated band structure. In this section, we proposed a model of the reconstructed FS, and discuss the origin of β and the characteristic behavior of the SdH oscillations.

A. Model of reconstructed Fermi surface in the SDW phase

From Table I, we note that there are significant relations between the observed frequencies: $F(\alpha_2) \approx F(\alpha_1) + F(\kappa)$,

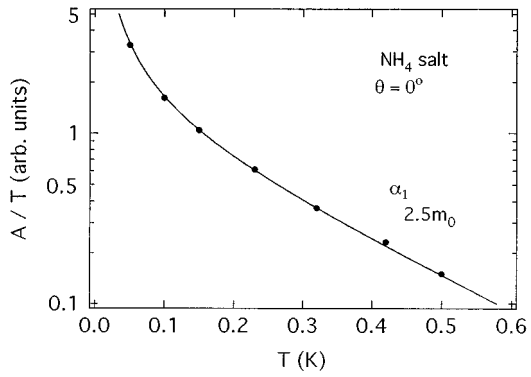

FIG. 13. Oscillation amplitude divided by temperature vs temperature for α_1 for the NH_4 salt. The solid line is the fitted result by the LK formula.

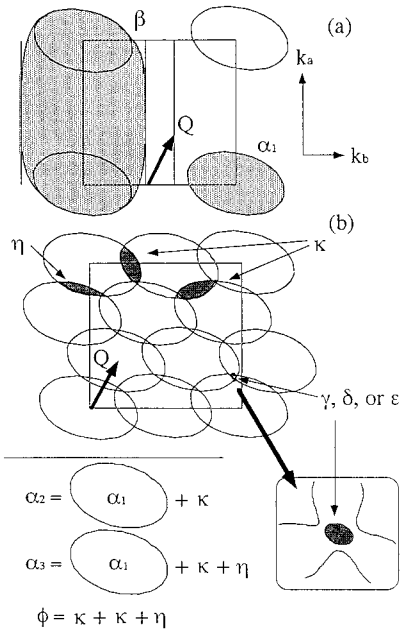

FIG. 14. (a) Schematic picture of the Fermi surface in the *M* phase. (b) Proposed reconstructed Fermi surface in the SDW. The nesting vector **Q** and the orbits assigned to the observed SdH oscillations are shown.

$F(\alpha_3) \approx F(\alpha_1) + F(\eta) + F(\kappa)$, and $F(\phi) = F(\eta) + 2F(\kappa)$. The first relation, for instance, suggests that the cyclotron orbit corresponding to the α_2 oscillation is formed by the combination of those corresponding to α_1 and κ. Taking account of the above frequency relations, we propose a possible structure of the reconstructed FS as shown in Fig. 14(b). The nesting vector Q is shown by the arrow. Some groups have proposed the models of the reconstructed FS, which have only one 2D FS and two sheets of the 1D FS in the new Brillouin zone.[19–22] However, our experimental results clearly show that the reconstructed FS has no 1D FS and is more complicated.

The smallest closed orbit is assigned to one of γ, δ, and ε. The six orbits corresponding to α_1, α_2, α_3, η, κ, and ϕ are the MB orbits. There are two possible orbits for α_2 and three possible ones for ϕ.[23] This reconstruction of the FS is consistent with the fact that all the oscillations have the same angular dependence. In Fig. 14(b), the nested 1D FS is not shown. Although two of γ, δ, and ε cannot be assigned to the orbits in this figure, it is likely that they arise from the small closed orbits formed by the imperfect nesting of the 1D FS.

The shape of the cross section of the original 2D FS in the ac plane has been investigated by the ADMRO measurements in the *M* phase for the K salt. The ADMRO observed in the *M* phase is well understood in terms of the geometrical property of the single weakly corrugated 2D FS.[30,31] Kovalev *et al.* measured the ADMRO above the transition temperature and found that the cross section of the 2D FS is elongated by a factor of ~1.5.[32] The longer axis of the ellipse is tilted from the *a* axis by ~30°. Caulfield *et al.* mapped out the 2D FS, which is elongated by a factor of ~2.[33] The longer axis of the ellipse is tilted from the *a* axis by ~50°. Sasaki and Toyota deduced an elongated 2D FS by a factor of ~1.5, whose longer axis is nearly parallel to the *a* axis.[20] At present, the shape of the 2D FS is still controversial. However, the ADMRO data in the *M* phase clearly shows that the cross section of the 2D FS has an elliptic shape. If we assume that the original 2D FS is elongated by a factor of ~1.6 and the longer axis is tilted from the *a* axis by ~20°, the observed oscillations are well reproduced [Fig. 14(b)]. The shape and area of the orbits corresponding to η, κ, and ϕ in Fig. 14(b) is very sensitive to the detailed shape of the original 2D FS. Although the model in Fig. 14(b) is still somewhat ambiguous, we can conclude that there are no open sheets of the 1D FS in the SDW phase. Without further precise measurements of the original 2D FS, it is impossible to determine the detailed structure of the reconstructed FS in the SDW phase.

The ADMRO observed in the SDW phase for the Tl, K, and Rb salts, which is very different from that for the NH_4 salt, has been explained in terms of the reconstructed 1D FS.[19–22] However, our results demonstrate that there are no open sheets of the 1D FS in the SDW phase. Recently, a theory of the ADMRO in the 2D system was proposed by Yoshioka.[34] He treated the 2D system under the tilted magnetic field and the periodic potential induced by the SDW formation, and calculated the effective hopping integral corresponding to the resistance along the b^* axis. The theory explains well the dip structure in the ADMRO. One of the important features in this theory is that the existence of the 1D FS is not necessarily assumed, which depends on the delicate balance between the size of the original FS and the SDW nesting vector. For the NH_4 salt, the standard ADMRO due to the 2D FS is also found.[19,21] The observed ADMRO is consistent with the single SdH oscillation.

B. Origin of the β oscillation

Here, we consider the origin of the β oscillation observed for the Tl, K, and Rb salts. The β oscillation is detected with α_1, α_2, α_3, and ϕ above ~7.5 T. When the original 1D FS is almost perfectly nested, β should not be measured.[35] The observation of β suggests that the original 1D FS shown in Fig. 14(a) exists in the magnetic field range below H_K. Therefore, it may be expected that at least two phases, the SDW phase having the reconstructed FS and the *M* phase having the original FS, coexist above ~7.5 T.

The kink behavior in the magnetoresistance at H_K is suppressed by the pressure.[4,12] The result shows that the SDW phase is removed under the pressure. Recently, Campos *et al.* report that the kink behavior is easily removed by the uniaxial pressure (~2 Kbar) along the b^*.[17] If some stress is locally present in the sample, the stressed part may have a lower critical field. In addition, if the local stress is distributed in a wide range, we can expect that the hysteretic behaviors in the magnetoresistance and the magnetization appear in a wide field range from a certain low field up to H_K because the phase transition is the first order. For the K salt, an additional phase line in the SDW state is proposed to exist at ~7 T from the observation of the large hysteresis in the magnetization and magnetoresistance above ~7 T.[3,20] In this case, the additional phase line at ~7 T corresponds to the field where the *M* phase partially appears. The coexistence of the *M* and SDW phases explains the hysteresis in the wide field range and the observation of β with α_1, α_2, α_3, and ϕ above ~7.5 T.

The characteristic ADMRO with the dip structure has been observed at fields from 1 T to $\sim H_K$ for the K or Tl salts, and the standard ADMRO arising from the 2D FS is not seen below $\sim H_K$.[19–22] The kink behavior in the magnetoresistance is evident only at $\sim H_K$. These facts suggest that the major part of the sample is in the SDW phase up to H_K ($\sim$23 T).

Recently, Harrison *et al.* reported the de Haas–van Alphen data measured by a pulse magnet for the K salt.[36] They observed the α_1 oscillation and its harmonics up to fourth in the field range between H_K and 54 T (M phase). However, the MB oscillation β was not seen within the experimental limits. They argue that there may be another mechanism for the β oscillation. Judging from their data, the amplitude of β is smaller than 3% of that of α_1 even if it exists. Along the MB orbit, there are four MB points. Therefore, the probability that the electrons travel along this orbit is given by p^4, where p is defined by Eq. (1). Similarly, the probability for the closed orbit (α_1) is given by $(1-p)^2$. Although the estimation of the MB field H_0 is somewhat ambiguous, it is expected to be in the range 30–100 T.[35] In this case, the ratio of the probability $p^4/(1-p)^2$ ranges from 0.1 to 0.0001 at 50 T. Therefore, even at 50 T, the relative oscillation amplitude of β to α_1 may be very small. We should note that the relative amplitude of β to α_1 is only $\sim$0.003 at 10.5 T (Fig. 8) and the oscillation amplitude is sample dependent. The absence of β in the pulse field data does not necessarily deny that β corresponds to the MB orbit.

C. Magnetic breakdown and resistance maximum at high magnetic field

The probability that the electrons travel along the cyclotron orbit corresponding to each oscillation is written as a function of the MB probability p in Eq. (1). The observation of α_1 and ϕ down to 4 T, which are assigned to the MB orbits [Fig. 14(b)], suggests that H_0 is comparable to 4 T at most. In the case of the reconstructed FS shown in Fig. 14(b), the probability that the electrons travel along the orbit assigned to α_1 is given by p^{12}, because 12 MB points are involved. This function smoothly increases with increasing field. On the other hand, the probability for other orbits assigned to α_2, α_3, ϕ, η, and κ include the Bragg reflection probability $(1-p)$, so that these oscillations should be suppressed at high fields. Therefore, in the SDW phase, only the α_1 oscillation is expected to dominate at high fields, which is consistent with the experimental results. It is very difficult to simulate the field dependence of the amplitude of each oscillation based on the reconstructed FS model because the oscillatory term of the conductivity includes unknown parameters.

We presented the in-plane resistance at 0.05 K for the Tl salt in Fig. 2. The nonoscillatory background of the resistance shows maxima around 11 T. Similar resistance maxima have been observed for the K and Rb salts but not observed for the NH_4 salt. As mentioned before, the large MB orbit (β) is evident for the Tl, K, and Rb salts having the SDW ground state. When the system has the 1D couples network composed of the 1D and 2D FSs as shown in Fig. 14(a), the conductivity tensor can be calculated by the path-integral method.[28,37] In the low-field limit, the MB is suppressed, so that the resistance rises quadratically with increasing field. In the high-field limit, the resistance decreases with increasing field where the MB dominates over the Bragg reflection at the zone boundary. Therefore, the resistance in the M phase is expected to have a maximum at a certain field and then decrease with increasing field above it. The field where the resistance has a maximum $H_{\max}$ increases and the maximum becomes broad as the scattering time becomes short. As the field is tilted from the b^* axis, the MB is suppressed because of the angular dependence of the energy gap and the effective mass. Therefore, $H_{\max}$ should increase as the field is tilted from the b^* axis as shown in the inset of Fig. 2. On the other hand, the resistance in the M phase is smaller than that in the SDW phase. The volume fraction of the M phase in the sample is expected to increase with increasing field above the additional phase line in the SDW phase. Therefore, if the two phases coexist, the negative slope of the resistance may be also caused by the field dependence of the volume ratio of the M phase to the SDW phase.

V. CONCLUSION

Many different SdH oscillations are found for $(BEDT\text{-}TTF)_2MHg(SCN)_4$ (M=Tl, K, and Rb) salts which have the SDW ground state. On the basis of the relation between the frequencies, the FS in the SDW phase is reconstructed. Our results show that the Tl, K, and Rb salts have the similar reconstructed FS, which has no open orbits. The reconstructed FS is more complicated than the models proposed by other groups. For the NH_4 salt, only one frequency is observed, which shows that the FS is not reconstructed. For M=Tl, K, and Rb, the β oscillation assigned to the MB orbit is observable, but not for the NH_4 salt. The result is understood in terms of the differences of the cross-sectional area of the 2D FS and the effective mass. The observation of β at high fields is probably due to the coexistence of the two phases, the M phase and the SDW phase. The anomalous temperature dependence of the nesting is found in the SDW phase for M=Tl and K.

ACKNOWLEDGMENTS

The experiments were done at Tsukuba Magnet Laboratories in NRIM. This work is partially supported by NSF DMR 92-14889.

[1] H. H. Wang, K. D. Carlson, U. Geiser, W. K. Kwok, M. D. Vashon, J. E. Thompson, N. F. Larsen, G. D. Mccabe, R. S. Hulscher, and J. M. Williams, Physica C **166**, 57 (1990).

[2] T. Sasaki and N. Toyota, Solid State Commun. **75**, 93 (1990); **75**, 97 (1990).

[3] T. Sasaki and N. Toyota, Solid State Commun. **82**, 447 (1992).

[4] J. S. Brooks, C. C. Agosta, S. J. Klepper, M. Tokumoto, N. Kinoshita, H. Anzai, S. Uji, H. Aoki, A. S. Perel, G. J. Athas, and

D. A. Howe, Phys. Rev. Lett. **69**, 156 (1992).
[5] N. D. Kushch, L. I. Buravov, M. V. Kartsovnik, V. N. Laukhin, S. I. Pesotskii, R. P. Shibaeva, L. P. Rozenberg, E. B. Yagubskii, and A. Z. Zvarikina, Synth. Met. **46**, 271 (1992).
[6] V. N. Laukhin, A. I. Shegolev, A. G. Khomenko, M. V. Kartsovnik, R. P. Shibaeva, L. P. Rosenberg, and A. E. Kovalev, Synth. Met. **55-57**, 1870 (1993).
[7] For definiteness, we describe the ground state as SDW. A detailed discussion of the ground state has recently been given, J. S. Brooks *et al.*, Proceedings of Physical Phenomena at High Magneic Fields—II, Tallahassee, Florida, 6–9 May, 1995, edited by Z. Fisk *et al.* (World Scentific, Singapore, in press).
[8] T. Sasaki, H. Sato, and N. Toyota, Synth. Met. **41-43**, 2211 (1991).
[9] H. Mori, I. Hirabayashi, S. Tanaka, T. Mori, H. Inokuchi, K. Oshima, and G. Saito, Synth. Met. **55-57**, 2443 (1993).
[10] N. Kinoshita, M. Tokumoto, and H. Anzai, J. Phys. Soc. Jpn. **59**, 3410 (1990).
[11] P. F. Henning, J. S. Brooks, J. E. Crow, Y. Tanaka, T. Kinoshita, N. Kinoshita, M. Tokumoto, and H. Anzai, Solid State Commun. **95**, 691 (1995).
[12] J. S. Brooks, S. J. Klepper, C. C. Agosta, M. Tokumoto, N. Kinoshita, Y. Tanaka, S. Uji, H. Aoki, G. J. Athas, X. Chen, and H. Anzai, Synth. Met. **55-57**, 1791 (1993).
[13] T. Osada, R. Yagi, A. Kawasumi, S. Kagoshima, N. Miura, M. Oshima, and G. Saito, Phys. Rev. B **41**, 5428 (1990).
[14] J. Singleton, F. L. Pratt, M. Doporto, T. J. B. M. Janssen, M. Kurmoo, J. A. A. J. Perenboom, W. Hayes, and P. Day, Phys. Rev. Lett. **68**, 2500 (1990).
[15] F. L. Pratt, J. Singleton, M. Doporto, A. J. Fisher, T. J. B. M. Janssen, J. A. A. J. Perenboom, M. Kurmoo, H. Hayes, and P. Day, Phys. Rev. B **45**, 13 904 (1992).
[16] H. Ito, H. Kaneko, T. Ishiguro, H. Ishimoto, and K. Kono, Solid State Commun. **85**, 1005 (1993).
[17] C. E. Campos, J. S. Brooks, P. J. M. van Bentum, J. A. A. J. Perenboom, S. J. Klepper, P. S. Sandhu, S. Valfells, Y. Tanaka, T. Kinoshita, N. Kinoshita, M. Tokumoto, and H. Anzai, Phys. Rev. B **52**, R7015 (1995).
[18] H. Mori, S. Tanaka, M. Oshima, G. Saito, T. Mori, Y. Murayama, and H. Inokuchi, Bull. Chem. Soc. Jpn. **63**, 2183 (1990).
[19] N. V. Kartsovnik, A. E. Kovalev, and N. D. Kushch, J. Phys. (France) I **3**, 1187 (1993).
[20] T. Sasaki and N. Toyota, Phys. Rev. B **49**, 10 120 (1994).
[21] Y. Iye, R. Yagi, N. Hanasaki, S. Kagoshima, H. Mori, H. Fujimoto, and G. Saito, J. Phys. Soc. Jpn. **63**, 674 (1994).
[22] J. Caulfield, S. J. Blundell, M. S. L. du Croo de Jongh, P. T. J. Hendriks, J. Singleton, M. Doporto, F. L. Pratt, A. House, J. A. A. J. Perenboom, W. Hayes, M. Kurmoo, and P. Day, Phys. Rev. B **51**, 8325 (1995).
[23] S. Uji, T. Terashima, H. Aoki, J. S. Brooks, M. Tokumoto, N. Kinoshita, T. Kinoshita, Y. Tanaka, and H. Anzai, J. Phys. Condens. Matter **6**, L539 (1994).
[24] T. Osada, A. Kawasumi, R. Yagi, S. Kagoshima, N. Miura, M. Oshima, H. Mori, T. Nakmura, and G. Saito, Solid State Commun. **75**, 901 (1990).
[25] J. S. Brooks, X. Chen, S. J. Klepper, S. Valfells, G. J. Athas, Y. Tanaka, T. Kinoshita, M. Tokumoto, H. Anzai, and C. C. Agosta, Phys. Rev. B **52**, 14 457 (1995).
[26] T. L. Sigfusson, K. P. Emilsson, and P. Mattocks, Phys. Rev. B **46**, 10 446 (1992).
[27] S. Uji, H. Aoki, M. Tokumoto, T. Kinoshita, N. Kinoshita, Y. Tanaka, and H. Anzai, Phys. Rev. B **49**, 732 (1994).
[28] D. Shoenberg, *Magnetic Oscillations in Metals* (Cambridge University Press, Cambridge, 1984).
[29] J. Wosnitza, G. W. Crabtree, H. H. Wang, K. D. Carlson, M. D. Vashon, and J. M. Williams, Phys. Rev. Lett. **67**, 263 (1991).
[30] K. Yamaji, J. Phys. Soc. Jpn. **58**, 1520 (1989).
[31] R. Yagi, Y. Iye, T. Osada, and S. Kagoshima, J. Phys. Soc. Jpn. **59**, 3069 (1990).
[32] A. E. Kovalev, M. V. Kartsovnik, R. P. Shibaeva, L. P. Rozenberg, and I. F. Schegolev, Solid State Commun. **89**, 575 (1994).
[33] J. Caulfield, J. Singleton, P. T. J. Hendriks, J. A. A. J. Perenboom, F. L. Pratt, M. Doporto, W. Hayes, M. Kurmoo, and P. Day, J. Phys. Condens. Matter **6**, L155 (1994).
[34] D. Yoshioka, J. Phys. Soc. Jpn. **64**, 3168 (1995).
[35] S. Uji, H. Aoki, J. S. Brooks, A. S. Perel, S. J. Klepper, C. C. Agosta, D. A. Howe, M. Tokumoto, N. Kinoshita, Y. Tanaka, and H. Anzai, Solid State Commun. **88**, 683 (1993).
[36] N. Harrison, A. House, I. Deckers, J. Caulfield, J. Singleton, F. Herlach, W. Hayes, M. Kurmoo, and P. Day, Phys. Rev. B **52**, 5584 (1995).
[37] L. M. Falicov and P. R. Sievert, Phys. Rev. Lett. **12**, 558 (1964); L. M. Falicov, A. B. Pippard, and P. R. Sievert, Phys. Rev. **151**, 498 (1966).